EFFECT OF MEAN STRESS ON FATIGUE STRENGTH OF TI -35NB-7ZR-5TA

Msc. FRANCO. H. A., pacific721031@yahoo.com
Dr. SILVA, C. R. M., cosmeroberto@gmail.com
Dr. FERREIRA, J. L. A, jorge@unb.br
Dra. MUTERLLE, P. V, pmuterlle@yahoo.com.br
Dr. ARAÚJO, J. A., alex07@unb.br
Eng. SANTOS, P. F., santos.fpedro@gmail.com
Universidade de Brasília, Faculdade de Tecnologia. UnB - Departamento de Engenharia Mecânica - Faculdade de Tecnologia - Campus Universitário. Asa Norte. 70910-900 - BRASILIA, DF - Brasil

Dr. HENRIQUES, V. A. R.,vinicius@iae.cta.br
Centro Técnico Aeroespacial, Iae. Praça Marechal-do-Ar Eduardo Gomes, 50 Vila das Acácias 12228-904 - São Jose dos Campos, SP - Brasil

Summary

The objective of this work is to evaluate the effect of mean stress on fatigue strength of Ti-35Nb-7Zr-5Ta, used in the manufacture of orthopedic prostheses. Twenty-three specimens were tested under four point bending fatigue conditions, and only fourteen specimens were considered with valid results, allowing to classify this research as exploratory. Specimens were prepared by powder metallurgy using elemental powders in the hydrogenated state. The elemental powders were mixed in a planetary mill, pressed by cold isostatic and uniaxial press and sintered for 3 hours at 1500°C in vacuum (10^{-7} Torr). For the material characterization the following techniques were used: optical microscopy, scanning electron microscopy, EDS analysis, oxygen analysis and density. The mechanical tests applied were microhardness (Vickers) and bending fatigue at four points. The microstructural analysis shows low densification after sintering (almost 86% of theoretical) and contain some precipitates of α phase and presumably ω phase at the grain and grain boundaries. The bending fatigue resistance limit found during the fatigue tests for the studied material was low ($S_e(10^6) = 90$ MPa), due to, presumably, the influence of the medium-high porosity, α phase precipitates at grain boundaries as well as the high oxygen content in the material after sintering (0.96 %). Finally, after building the equivalent mean stress curve versus number of cycles considering several models that quantify the effect of mean stress, it was concluded that the model of Kwofie is the one that best explains the influence of mean stress on fatigue strength of this alloy.

Keywords: *Ti -35Nb-7Zr-5Ta, Mean stress, four point bending fatigue, Powder metallurgy*

1. INTRODUCTION

The use of Powder Metallurgy (P/M) aims to obtain orthopedic implants with almost net-shaping and adequate mechanical properties and surface porosity. The surface porosity is necessary to improve an efficient interaction between the implant and the bone (Medeiros *et al.* 2005).

The control and quantification of porosity is very important because its size and morphology are essential to the cellular adhesion. It is necessary to obtain a high porosity to improve bone-formation inside the pores (Oliveira *et al.* 2005).

Sintering is irreversible, so a perfect control during the process is necessary. After the sintering, alternative technologies are used to modify some properties, to improve the shape or dimensional accuracy so as to extend the range of application (German, 1996).

The lower modulus β Ti alloys have been developed recently because they exhibit a modulus near of bone modulus and those alloys have other desired properties like ideal bio-alloy. Biomedical alloys needs a good relation between low modulus and enough strength and alloying additions that are biocompatible (Banerjee *et al.* 2005). The P/M Ti 35Nb 7Zr 5Ta alloy (TNZT) with 55 GPa modulus is considered one of the best to be used as a orthopedic implant. This TNZT has excellent non-toxic components with good mechanical properties and workability. (Niinomi, 2003; Katti, 2004; Geeta *et al.* 2004)

The recent trend in research and development of titanium alloys for biomedical applications is to develop low rigidity β type titanium alloys composed of non-toxic and non-allergic elements with excellent mechanical properties and workability (Niinomi, 2002) According to this concept, different new β type have been developed like Ti–29Nb–13Ta–4.6Zr (Kuroda *et al.* 1998; Niinomi *et al.* 1999; Kuroda et al, 2001; Akahori *et al.* 2001) and Ti 35Nb 7Zr 5Ta obtained just by P/M (Taddei, 2007) alloy composed of elements like Nb, Ta, and Zr (Steinemann, 1980; Kawahara *et*

al. 1963) for biomedical applications. It is still necessary to evaluate various performances of Ti–35Nb–7Zr-5Ta for practical use.

Fatigue performance is one of the most important mechanical performances for biomaterials because, in general, biomaterials are used under cyclic loading. Fatigue performance of titanium alloy varies according to mean stress applied. The influence of mean stress on fatigue strength of the new β type titanium alloy M/P obtained, Ti 35Nb 7Zr 5Ta, were investigated in relation with microstructures in this study.

1.1. Basic relations of load characterization

The fatigue life is described by the Wöhler curve or *S-N* curve, Stress-Life, where the number of cycles to failure, *N*, is correlated with the alternating stress, S_a. This method is a relation that can be well used to adjust appropriately experimental data in the sense to correlate the alternate stress and the number of cycles to failure between 10^3 and 10^6 cycles. This relation can be expressed as in Eq. (1), where *A* and *b* are the constant and the curve exponent, respectively.

$$S_a = A \cdot N^b \tag{1}$$

Some practical applications and also fatigue tests in materials involve maximum and minimum level stresses that characterize the amplitude loads. The stress range, Δ*S*, is the difference between the maximum value and minimum value, Eq. (2). The mean stress, S_m, is the average between maximum value and minimum value, Eq. (3). The half of the range stress is called amplitude stress, S_a, Eq. (4). These are basic relations that characterize one load cycle.

$$\Delta S = S_{max} - S_{min} \tag{2}$$

$$S_m = \frac{S_{max}+S_{min}}{2} \tag{3}$$

$$S_a = \frac{S_{max}-S_{min}}{2} \tag{4}$$

And to describe the mean stress, a factor used to characterize the degree of symmetry of the load, load ratio, *R*, is defined by Eq. (5). The relation between S_a, S_m and *R* is expressed in the Eq. (6).

$$R = \frac{S_{min}}{S_{max}} \tag{5}$$

$$S_a = \frac{1+R}{1-R} S_m \tag{6}$$

The standard condition to determine the parameters of Wöhler curve is to assume alternating load, null mean stress. Thus, the Eq. (1) can be expressed in the form of Eq. (7). It is called Basquin's equation. Where σ_f' and *b* are material constants based in experimental results.

$$S_{ar} = \sigma_f' N^b \tag{7}$$

1.2. Mean stress effect prediction models

Initially, empiric models were proposed by Gerber (1874), Goodman (1899), Haigh (1917) and Soderberg (1930) to compensate the effect of mean stress in the high cycle fatigue strength. Gerber proposed a parabolic representation of the Wöhler's limit fatigue data on the graphic S_{max}/S_u *versus* S_{min}/S_u , Eq. (12). Goodman introduced a theoretical line to represent the evaluated fatigue data, Eq. (11). Haigh was the first to plot the fatigue data in the graphic S_a *versus* S_m. starting around 1960, some models to determine the effect of mean stress have been proposed as improvements of the previous models. Fatigue tests indicate that the tensile normal mean stress should reduce the fatigue strength coefficient and that the compressive normal mean stress should increase it (Lee *et al.* 2005).

In order to overcome the failure prediction's problem under load conditions with relatively low amplitude and relatively high mean stresses, Smith, Watson and Topper - SWT (Smith *et al.* 1970) proposed a model in which the equivalent stress to the endurance limit for the load ratio, *R* = -1, S_{ar}, is expressed in the Eq. (13). On this same year, Walker (1970) presented criteria similar to SWT, however using a factor γ that makes possible an adjustment of the curve in relation to the experimental data, Eq. (14). According to empiric data, Berkovits and Fang (Berkovits *et al.* 1993) and more recently Kwofie (2001) proposed widespread mathematical relations to describe the effect of mean stress on the fatigue behavior of endurance limit. Such model consists in the substitution of the Basquin's equation's constant, Eq. (7), for a function that will depend on the mean stress, S_m, on the limit of fatigue strength for the reverse load condition, S_{rt}, and on the ultimate strength, or yield strength, S_y. According to this model, the stress-life relation can be presented by Eq. (8).

$$\sigma_a = S_{ar} e^{\left(-\alpha \frac{\sigma_m}{S_{rt}}\right)} \quad (8)$$

Expressed in form of power series, the Eq. (8) can be expressed by Eq. (9):

$$\sigma_a = S_{ar} e^{\left(-\alpha \frac{\sigma_m}{S_{rt}}\right)} \cong \sum_{i=0}^{N} \cdot \frac{1}{i!} \cdot \left(-\alpha \frac{\sigma_m}{S_{rt}}\right)^i \quad (9)$$

Admitting that the argument of the exponential function tends to zero, α $(\sigma_m/S_{rt}) \rightarrow 0$, the consequence is that the terms of superior order converge quickly to zero. In this specific condition, the Eq. (9) assumes the following form:

$$\sigma_a \cong S_{ar} \left(1 - \alpha \frac{\sigma_m}{S_{rt}}\right) \quad (10)$$

Starting from this last expression, one can verify easily that depending on the value of α, the widespread model will describe some models presented in the Tab. (1).

Table 1. Particular solutions of widespread Kwofie model. (Oliveira *et al.* 2009).

Hypothesis	*Resulting Equation*	*Model*	*Equation*
α=1	$\frac{\sigma_a}{\sigma_{ar}} + \frac{\sigma_m}{\sigma_{rt}} = 1$	Goodman	(12)
$\alpha = f\left(\frac{\sigma_m}{S_{rt}}\right) = \frac{\sigma_m}{S_{rt}}$	$\frac{\sigma_a}{\sigma_{ar}} + \left(\frac{\sigma_m}{\sigma_y}\right)^2 = 1$	Gerber	(13)
$\alpha = f(R, S_{rt,} \sigma_m) = -\frac{S_{rt}}{\gamma \sigma_m} ln\left(\frac{1-R}{2}\right)$	$\sigma_a = S_{ar}\left(\frac{1-R}{2}\right)^{\gamma}$	*Walker*	(14)
$\alpha \frac{\sigma_m}{S_{rt}} \rightarrow 0$	$S_{ar} = \frac{\sigma_a}{1 - \alpha \frac{\sigma_m}{S_{rt}}}$	Kwofie	(15)

2. MATERIALS AND METHODS

For the preparation of the alloy, the blended elemental method followed by a sequence of uniaxial and cold isostatic pressing with subsequent densification by sintering was chosen. All the powders were obtained by hydriding method and sintered in hydride state. The starting powders were weighed and dried for one hour in stove and blended for 30 minutes in a planetary mill. After blending, the powders were cold uniaxially pressed under pressure of 60 MPa. Afterwards, samples were encapsulated under vacuum in flexible rubber molds and cold isostatically pressed (CIP) at 350 MPa during 30 seconds in an isostatic press. Sintering was carried out in niobium crucible in high vacuum condition (10^{-7} Torr), at 1500 °C.

Metallographic preparation was carried out using conventional techniques. Specimens were etched with a Kroll solution: 1.5 *ml* HF: 2.5 ml HNO_3: 100 *m*l H_2O, for 50 seconds, to reveal its microstructure. Microhardness measurements were carried out in a PANTEC Micrometer with a load of 200g for 20 seconds (15 indentations). The micrographs were obtained using a SEM Philips Quanta model 200 3D and optic microscope "OLYMPUS BX51. The porosity was determinate by the Arquimedes method. The analysis of oxygen and nitrogen was made in the Material's Lab at University of Trento.

Bending fatigue at four points was conducted in a universal testing machine MTS 810. Figure 1 illustrates the specimens' positioning and distances of points of contact with the machine. Testing loads were found using Eq. (11), which derives from a simple free body diagram, and stress values as found in Table 3. Tests were conducted at a frequency of 20 Hz.

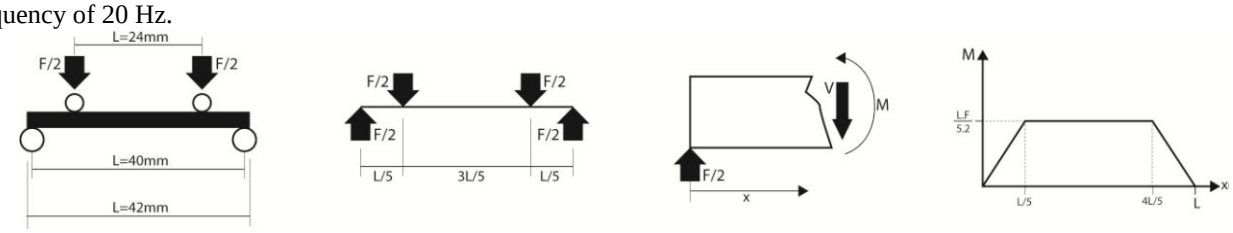

1 2 3 4

Figure 1. 1. Schematic representation of test conditions 2. Free body diagram 3. Simplified diagram of internal forces 4. Bending moment diagram for test conditions.

$$F = \frac{\sigma \cdot b \cdot h^2}{24 \cdot 10^3} \quad (11)$$

2.1 Material

The material used in the development of this research was the Ti 35Nb 7Zr5 Ta alloy, a β titanium alloy. This is a new biocompatible alloy used in the production of orthopedic implants. The mechanical properties (Young modulus (*E)*, tensile strength, S_{rt}, and yield strength, S_y), oxygen and nitrogen content, density and densification of the alloy are summarized in Table 2.

Table 2 Mechanical properties of Ti 35Nb 7Zr 5Ta.

Alloy	kind	Srt (MPa)	Sy (MPa)	E (MPa)	O%	N%	Density [g/cm^3]	Densification [%]
Ti35Nb7Zr5Ta	**β**	**596.5**	**547.1**	**55**	**0.96**	**0.0111**	**5.60±0.05**	**85**

3. RESULTS AND DISCUSSION

3.1 Microstructure

In the microstructure presented in Figure 2 we can see a β-homogeneous microstructure with relative high porosity. Due to the complete dissolution of the alloys elements in the titanium matrix, a good combination of microstructure, mechanical properties and desired densification could be reached.

The samples sintered at 1500 °C presented a β-homogeneous microstructure with medium porosity. The alloy presented microhardness values around 340 HV, next to the observed in samples produced by the melting conventional method (Allvac, 2002). The microstructure, observed in optical and SCAN microscope, of the TNZT alloy in the sintered condition are shown in the Figure 2and Figure 3. The microstructure consists of relatively large grains of phase β with grain boundary α precipitates. In addition, some amount of intra-granular α precipitation is also visible within β grains. These intra-granular primaries α precipitates often exhibit rather different morphologies (plates and needles).

The Figure 3 allows to see α and β areas (sintered at 1500^{o}C) where the analyses for EDS were carried out. Areas 1 and 2 are, preferably, β and α region respectively.

The medium porosity presence, area 3 (observed in Figure 3a) is an important feature for osseointegration, when aiming for surgical implants application, where a medium-high porosity is necessary. An efficient route to control the pore content in TNZT samples is selecting an adequate space holder. This sintering method in order to manufacture highly porous metallic materials was investigated in other research, (Taddei, 2007).

In the figure 3b are signalized (region 4) the probably ω phase, these precipitate will be certainly identified through the Transmission Electron Microscopy and will be published in future papers. It is possible that the same precipitate would be formed into the grain boundary.

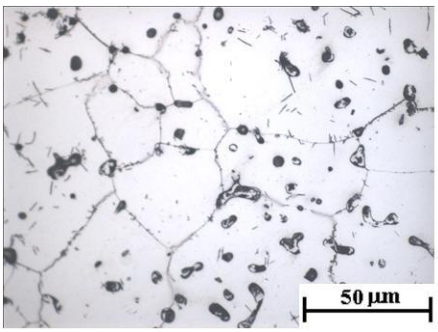

Figure 2. Optic microstructure of sintered Ti 35Nb 7Zr 5Ta alloy a)200x b) 500x

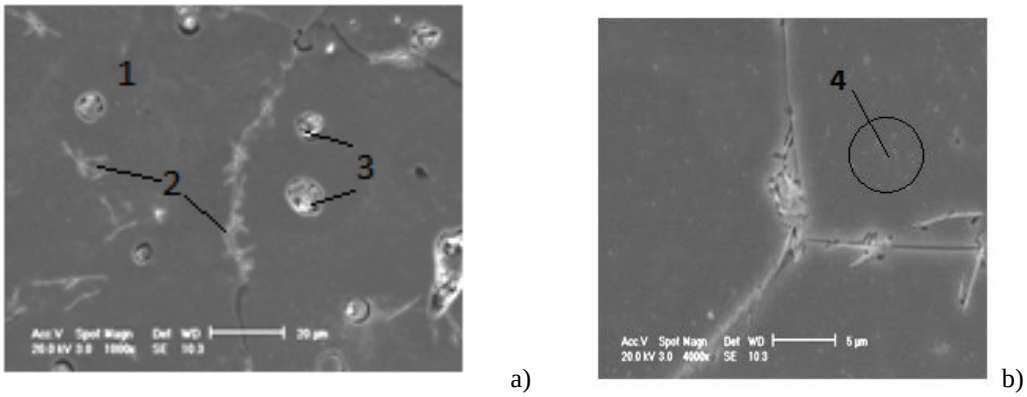

Figure 3. Electronic Scan Microstructure of sintered Ti 35Nb 7Zr 5Ta alloy a)1000x b) 4000x

The EDS analyses represent the compositions of the alloy elements in the graphic showed in figure 4. It is possible to observe the alloyed element distribution into the β matrix.

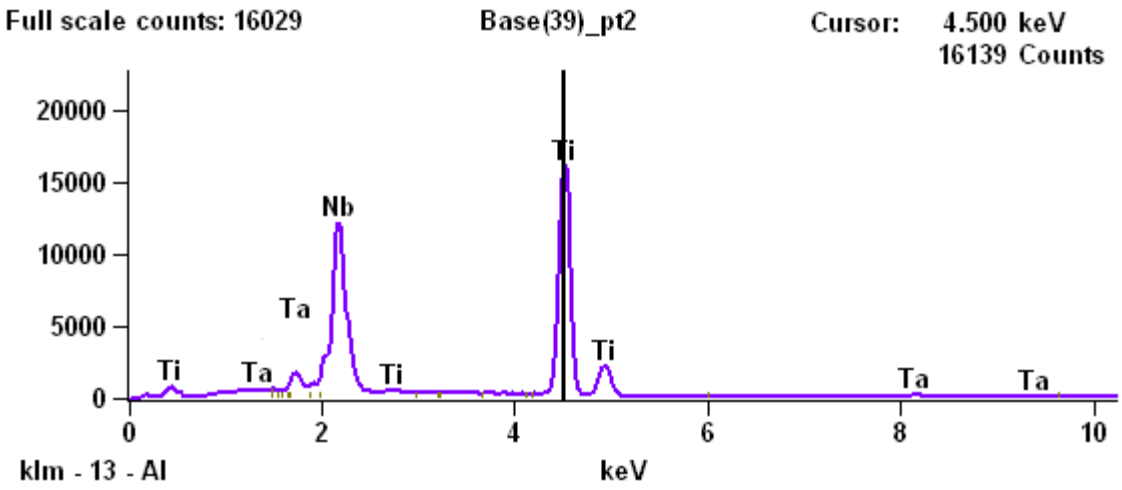

Figure 4. EDS analysis in the matrix area.

3.2 S-N curve test

The test stress conditions, the load ratio, R, used on the four bending fatigue tests as well as, the number of cycles to failure, N, obtained are shown in table 3.

Table 3. Mean and alternate stress, R applied on four bending fatigue tests and N obtained.

	σ_{alt}	σ_{med}	R	N
CP1	215.6	264.4	0.1	9.48E3
CP2	185.7	233.7	0.1	1.60E4
CP3	162.9	198.6	0.1	2.42E4
CP4	133.6	163.7	0.1	2.28E5
CP5	96.7	118.7	0.1	2.99E5
CP6	90.6	112.2	0.1	2.20E5
CP7	95.0	116.6	0.1	6.45E5
CP8	84.8	258.9	0.5	1.36E6

	σ_{alt}	σ_{med}	R	N
CP9	102.6	248.0	0.4	1.44E6
CP10	112.5	337.5	0.5	2.44E5
CP11	155.4	241.4	0.3	9.34E4
CP12	157.5	292.5	0.3	5.42E4
CP13	157.8	192.9	0.1	1.7E4
CP14	202.5	247.5	0.1	4.47E3

Figure 5 shows the linearization obtained through the electronic spreadsheet software, based on the experimental data of fatigue test in alternated stress and Figure 6 shows the adjustment of the experimental data considering a Mono-log linearization. Based on test result was found that the fatigue strength of this alloy for this sintered condition is approximately $S_e^{'}$= 90MPa.

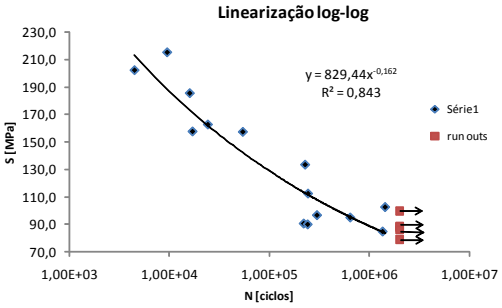

Figure 5. Log-log Linearization

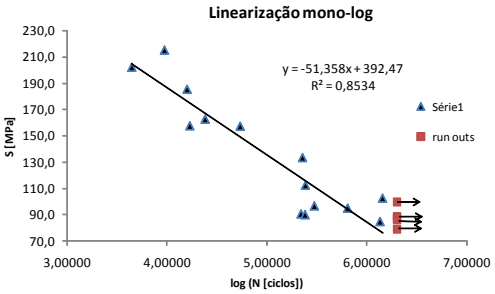

Figure 6. Mono-log Linearization

3.3 Effect of mean stress

Considering the goal of this work, it is necessary check the adherence of the Goodman, Gerber, Kwofie and Walker´s models making a comparison between the results and obtained graphics with the results of the S-N linearization results. Since the S-N graphics don't include the mean stress effect it is necessary standardized the equivalent alternated stress through the models based on expressions in table 1, for Goodman:

$$\sigma_a = \left(\frac{\sigma_{alt}}{1-\sigma_{med}/S_{rt}}\right) \tag{12}$$

Once found, the equivalent alternated stress using Eq. (12) takes in consideration the experimental mean stress. For each point, the S_{ar}-N relation was obtained for Goodman model, considering the adherence of log-log and mono-log relations.

Figure 7 shows the log-log linearization obtained for Goodman model based in the experimental results. In Figure 8 it is possible to observe the mono-log linearization for Goodman model based in the experimental results.

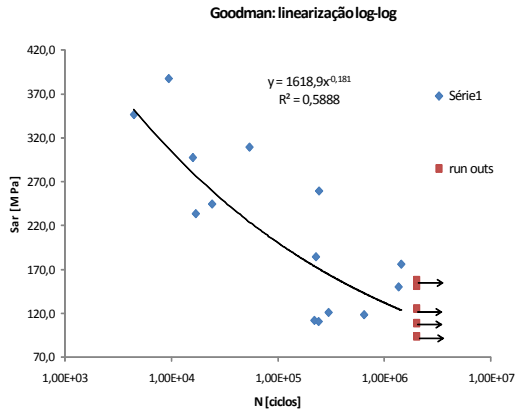

Figure 7. Goodman model adjustment log-log

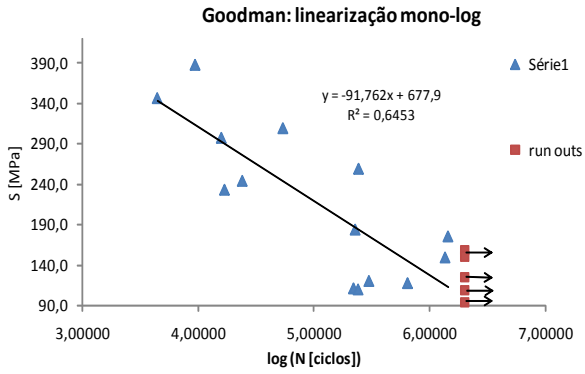

Figure 8. Goodman model adjustment mono-log

For Gerber model:

The eq. (13) was used to calculate equivalent alternated stress at the Gerber Model and the associated graphics were plotted. Figure 9 shows the log-log linearization obtained for the Gerber model using the experimental data and in figure 10 it is possible to see the mono-log linearization for Gerber model plotted with the experimental data.

$$\sigma_a = \left(\frac{\sigma_{alt}}{1-(\sigma_{med}/S_{rt})^2}\right) \quad (13)$$

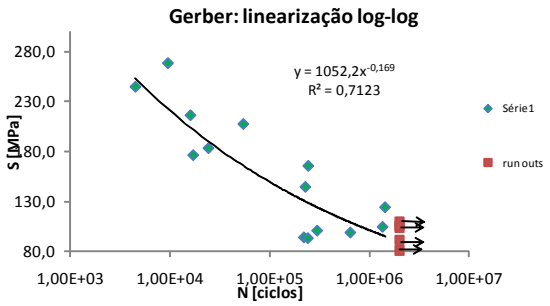

Figure 9. Gerber model adjustment log-log

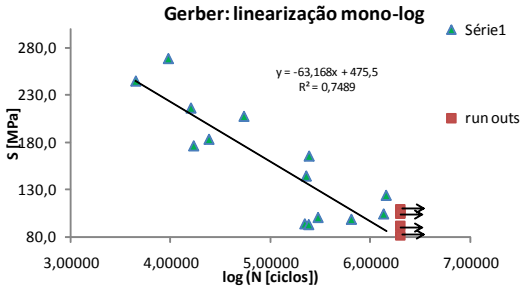

Figure 10. Gerber model adjustment mono-log

For Walker model:

The eq. (14) was used to calculate equivalent alternated stress for the Walker Model and the associated graphics were plotted.

Figure 11 shows the log-log linearization obtained for the Walker model using the experimental data and in Figure 12 one observe the mono-log linearization for Walker model based in the experimental results.

$$S_{ar} = \sigma_a \cdot \left(\frac{2}{1-R}\right)^{1-\gamma} \quad (14)$$

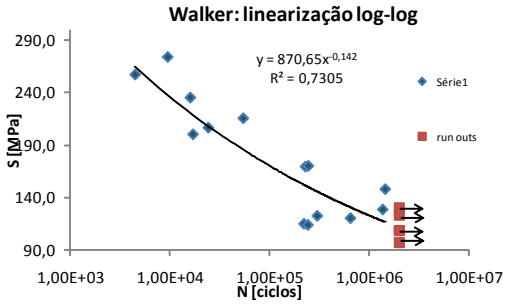

Figure 11.Walker model adjustment log-log

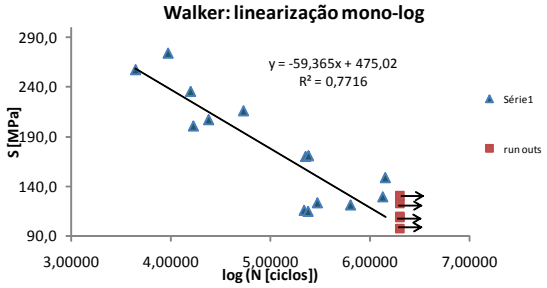

Figure 12. Walker model adjustment mono-log

For Kwofie model:

Using the Eq. (15) the equivalent alternated stress was calculated for Kwofie Model and the associated graphics were plotted.

Figure 13 shows the log-log linearization obtained for the Kwofie model using the experimental data and Figure 14 permit appreciated the mono-log linearization for Kwofie model based in the experimental results.

$$S_{ar} = \frac{\sigma_a}{1-\alpha\frac{\sigma_m}{S_{rt}}} \quad (15)$$

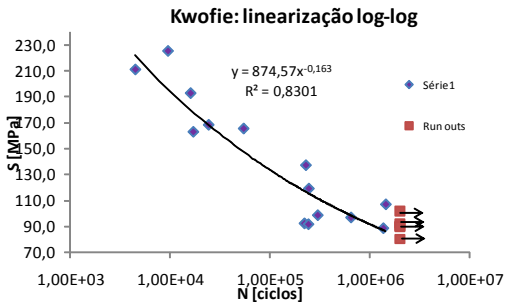

Figure 13. Kwofie model adjustment log-log.

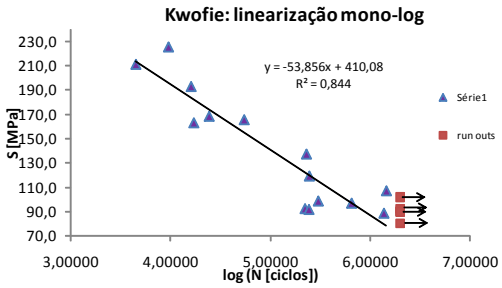

Figure 14. Kwofie model adjustment mono-log

3.4 Models comparison

A summary of the R^2 (log-log) and $*R^2$ (mono-log) results of the studied models could be compared in table 4.

Table 4 Determination Coefficients of the studied models

	S-N	Goodman	Gerber	Walker	Kwofie
R^2	0.8466	0.6427	0.7531	0.7378	0.8346
$*R^2$	0.8561	0.7017	0.7780	0.7746	0.8461

The S-N column represents the analysis without the influence of the mean stress effect; apparently it is who better explain the material behavior. Was analyzed, based in Kwofie criteria when $\alpha \rightarrow 0$ the material mean stress sensibility tend to be lower. Considering the experimental results the Ti 35Nb 7Zr 5Ta alloy showed big mean stress insensibility. The mono-log linearizations show us a better adherence to the experimental data and hence, are the models who offer us a better analysis of the statistical test results. The results analysis using the ASTM E739 show that S-N curve without the incidence of mean stress and Kwofie model presents better confidence rate even in the more dispersed points.

Kwofie and Walker showed themselves like the more dynamics models (reminding that for $\gamma = 0.7$ Walker and Gerber have the same behavior) its tend is a good adherence to the experimental data.

4. CONCLUSIONS

The aim of this research was to evaluate the effect of mean stress on the fatigue behavior of Ti 35Nb 7Zr 5Ta alloy. In that sense, *S-N* curves were experimentally determined for different stress values. Results obtained allow only for a qualitative study, being this an exploratory research. The results were used to determine the endurance limit of the material and to evaluate the predictions of such models. The Goodman, Gerber, Walker and Kwofie's models were used to predict the mean stress effects. Through the analysis of the test results it is possible to conclude that: a) the fatigue strength limit for this sintered TNZT alloy is approximately S_e(10E6) = 90 MPa analytically obtained; b) the fatigue strength is not strongly influenced by the presence of mean stresses; c) Goodman model was shown inadequate to describe the statistical test results of mean stress effect on the fatigue strength; d) Gerber and Walker's model presents a reasonable prediction for the presence of mean stress; e) Kwofie's model was the model to best describe the effect of the mean stress on the fatigue strength of Ti 35Nb 7Zr 5Ta alloy. Through the micrograph analysis, relatively medium-high porosity was determined; that's necessary for a good osseointegration. Nevertheless, those pores could affect the mechanical properties, hence, should be controlled. At β matrix, and even at grain boundary, precipitates were found, presumably α and/or ω phase. Possibly the high content of oxygen, the 14% of porosity and grain-boundary precipitates are responsible for the low fatigue strength limit.

5.REFERENCES

Akahori, T., Niinomi, M., Yabunaka, T., Kuroda, D., Fukui, H., Suzuki, A., Hasegawa, J., 2001. Fretting fatigue characteristics of biomedical new b titanium alloy, Ti–29Nb–13Ta–4.6Zr.In: Hanada, S., Zhong, Z., Nam, S. W., Wright, R. N., editors. Proceedings of the PRICM 4: The Jpn. Inst. Metals, p. 209–12.

Allvac, 2002. An Allegheny Technologies Company, Catalogue.

ASTM / E 739-91, 1991. "Standard Practice for Statistical Analysis of Linear or Linearized Stress-Life (S-N) and Strain-Life (e-N)".

Banerjee, R., Nag, S., Fraser, H., 2005. A novel combinatorial approach to the development of beta titanium alloys for orthopaedic implants. Materials Science and Engineering C; 25:282-289.

Berkovits, A., Fang, D., 1981. "An analytical master curve for Goodman diagram data", Int. J. Fatigue, 15, pp. 173-80.

Gill, P. R., Murray, W., Wright, M. H., 1993. "The Levenberg-Marquardt Method" in Practical Otimization, London: Academic Press, pp. 136-137.

Medeiros, W. S., Oliveira, M. V., Pereira, L. C., Cairo, C. A. A., Calixto, M. A., 2005. Calcium Phosphate Deposition on Porous Titanium Samples. In Fifth International Latin-American Conference on Powder Technology, 2005, Costa do Sauipe. Procedings of Fifth International Latin-American Conference on Powder Technology; Metallum Eventos Técnicos Científicos, Bahia, Brazil, v. CD.

Geetha, M., Kamachi, M. U., Gogia, A. K., Asokamani, R., Raj, B., 2004. Influence of microstructure and alloying elements on corrosion behavior of Ti–13Nb–13Zr alloy. Corrosion Science; 46(4):877-892.

German, M. R., 1996. Sintering Theory and practice. By Jhon Wiley & sons, inc.

Katti, K. S., 2004. Biomaterials in total joint replacement, Colloids and Surfaces B. Biointerfaces 39 (3):133-142.

Kawahara, H., Ochi, S., Tanetani, K., Kato, K., Isogai, M., Mizuno, Y., Yamamoto, H., Yamaguchi, A., 1963. Biological test of dental materials, Effect of pure metals upon the mouse subcutaneous fibroblast, strain L cell in tissue culture. J. Jpn. Soc. Dent. Apparat. Mater; 4:65–75.

Kwofie, S., 2001. "An exponential stress function for predicting fatigue strength and life due to mean stresss", Int. J. Fatigue, 23, pp. 829-836.

Kuroda, D., Niinomi, M., Fukui, H., Suzuki, A., Hasegawa, S., 2001. Mechanical performance of newly developed β - type titanium alloy, Ti–29Nb–13Ta–4.6Zr, for biomedical applications. In: Niinomi, M., Okabe, T., Taleff, E. M., Lesure, D. R., Lippard, H. E., editors. Structural biomaterials for the 21st century. Warrendale: TMS, p. 99–106.

Kuroda, D., Niinomi, M., Morinaga, M., Kato, Y., Yashiro, T. 1998. Design and mechanical properties of new β type titanium alloys for implant materials. Mat. Sci. Eng. A; A 243:244–9.

Lee, Y-L., Pan, J., Hathaway, R., Barkey, M. E., 2005. "Fatigue Testing and Analysis (Theory and Practice)", Elsevier Butterworth-Heinemann, USA.

Niinomi, M., 2003. Fatigue performance and cytotoxicity of low rigidity titanium alloy, Ti-29Nb-13Ta-4.6Zr. Biomaterials. 24 (16):2673-2683.

Niinomi, M., 2002. Recent metallic materials for biomedical applications. Metal Mater. Trans. A; 33A:477–86.

Niinomi, M., Kuroda, D., Fukunaga, K., Morinaga, M., Kato, Y., Yashiro, T., Suzuki, A., 1999. Corrosion wear fracture of new β type biomedical titanium alloys. Mat. Sci. Eng. A; A263: 193–9.

Oliveira, F., Ferreira, J. L. A., Araújo, J. A., 2009. Determinação da Resistência à Fadiga do Aço ASTM A743 - CA6NM - Tomo 3 - Efeito da Presença da Tensão Média Sobre a Vida em Fadiga. Universidade de Brasília.

Oliveira, M. V., Moreira, A. C., Appoloni, C. R., Lopes, R. T., Pereira, L. C., Cairo, C. A. A., 2005. Porosity Study of Sintered Titanium Foams. In Fifth International Latin-American Conference on Powder Technology, Costa do Sauipe. Procedings of Fifth International Latin-American Conference on Powder Technology; Metallum Eventos Técnicos Científicos, Bahia, Brazil.

Steinemann, S. G., 1980. Corrosion of surgical implants in vivo and in vitro tests. In: Winter, G. D., Leray, J. L., De Groot K, editors. Evaluation of biomaterials. NewYork: Wiley, p. 1–34.

Smith, K. N., Watson, P., Topper, T. H., 1970. "A Stress Strain Function for the Fatigue of Metals", Journal of Materials, ASTM, Vol. 5, No. 4, 99. 767 – 778.

Taddei, E. B., 2007. Obtenção da liga Ti 35Nb 7Zr 5Ta por metalurgia do pó para utilização em próteses ortopédicas. Tesis de Doutorado. Campo Montenegro, São José dos Campos, SP- Brasil.

Walker, K., 1970. "The Effect of Stress Ratio During Crack Propagation and Fatigue for 2024-T3 and 7075-T6 Aluminum", Effect of Environment and Complex Load History on Fatigue Life, ASTM STP 462, Am. Soc. For Testing and Materials, West Conshohocken, PA, pp. 1-14.

6. RESPONSIBILITY NOTICE

The authors are the only responsible for the printed material included in this paper.